A wide, flat, gravelly beach stretches across the foreground and middle ground, meeting a calm body of water on the left. The background features a dense line of green trees and some buildings under a clear blue sky with a few wispy clouds. The overall scene is bright and clear, suggesting a sunny day.

# EXPLAINING EXTREME EVENTS OF 2018

## From a Climate Perspective

Special Supplement to the  
*Bulletin of the American Meteorological Society*  
Vol. 101, No. 1, January 2020

# EXPLAINING EXTREME EVENTS OF 2018 FROM A CLIMATE PERSPECTIVE

## **Editors**

Stephanie C. Herring, Nikolaos Christidis, Andrew Hoell,  
Martin P. Hoerling, and Peter A. Stott

## **BAMS Special Editors for Climate**

Andrew King, Thomas Knutson,  
John Nielsen-Gammon, and Friederike Otto

## **Special Supplement to the**

*Bulletin of the American Meteorological Society*

Vol. 101, No. 1, January 2020

**AMERICAN METEOROLOGICAL SOCIETY**

CORRESPONDING EDITOR:

Stephanie C. Herring, PhD  
NOAA National Centers for Environmental Information  
325 Broadway, E/CC23, Rm 1B-131  
Boulder, CO, 80305-3328  
E-mail: [stephanie.herring@noaa.gov](mailto:stephanie.herring@noaa.gov)

COVER CREDIT: iStock.com/Alena Kravchenko—River Thames receded during a heatwave in summer 2018 in London, United Kingdom.

HOW TO CITE THIS DOCUMENT

---

Citing the complete report:

Herring, S. C., N. Christidis, A. Hoell, M. P. Hoerling, and P. A. Stott, Eds., 2020: Explaining Extreme Events of 2018 from a Climate Perspective. *Bull. Amer. Meteor. Soc.*, **101** (1), S1–S128, doi:10.1175/BAMS-ExplainingExtremeEvents2018.1.

Citing a section (example):

Mahoney, K., 2020: Extreme Hail Storms and Climate Change: Foretelling the Future in Tiny, Turbulent Crystal Balls? [in “Explaining Extremes of 2018 from a Climate Perspective”]. *Bull. Amer. Meteor. Soc.*, **101** (1), S17–S22, doi:10.1175/BAMS-D-19-0233.1.

## TABLE OF CONTENTS

1. The Extreme 2018 Northern California Fire Season . . . . .	1
2. Anthropogenic Impacts on the Exceptional Precipitation of 2018 in the Mid-Atlantic United States . . . . .	5
3. Quantifying Human-Induced Temperature Impacts on the 2018 United States Four Corners Hydrologic and Agro-Pastoral Drought . . . . .	11
4. Extreme Hail Storms and Climate Change: Foretelling the Future in Tiny, Turbulent Crystal Balls? . . . . .	17
5. The Extremely Cold Start of the Spring of 2018 in the United Kingdom . . . . .	23
6. The Exceptional Iberian Heatwave of Summer 2018 . . . . .	29
7. Analyses of the Northern European Summer Heatwave of 2018 . . . . .	35
8. Anthropogenic Influence on the 2018 Summer Warm Spell in Europe: The Impact of Different Spatio-Temporal Scales . . . . .	41
9. On High Precipitation in Mozambique, Zimbabwe and Zambia in February 2018 . . . . .	47
10. The Record Low Bering Sea Ice Extent in 2018: Context, Impacts, and an Assessment of the Role of Anthropogenic Climate Change . . . . .	53
11. The Late Spring Drought of 2018 in South China . . . . .	59
12. Anthropogenic Influence on 2018 Summer Persistent Heavy Rainfall in Central Western China . . . . .	65
13. Conditional Attribution of the 2018 Summer Extreme Heat over Northeast China: Roles of Urbanization, Global Warming, and Warming-Induced Circulation Changes . . . . .	71
14. Effects of Anthropogenic Forcing and Natural Variability on the 2018 Heatwave in Northeast Asia . . . . .	77
15. Anthropogenic Influences on the Persistent Night-Time Heat Wave in Summer 2018 over Northeast China . . . . .	83
16. Anthropogenic Contributions to the 2018 Extreme Flooding over the Upper Yellow River Basin in China . . . . .	89
17. Attribution of the Record-Breaking Consecutive Dry Days in Winter 2017/18 in Beijing . . . . .	95
18. Quantifying Human Impact on the 2018 Summer Longest Heat Wave in South Korea . . . . .	103
19. The Heavy Rain Event of July 2018 in Japan Enhanced by Historical Warming . . . . .	109
20. Deconstructing Factors Contributing to the 2018 Fire Weather in Queensland, Australia . . . . .	115
21. A 1-Day Extreme Rainfall Event in Tasmania: Process Evaluation and Long Tail Attribution . . . . .	123



THE EXCEPTIONAL IBERIAN HEATWAVE  
OF SUMMER 2018

D. BARRIOPEDRO, P. M. SOUSA, R. M. TRIGO, R. GARCÍA-HERRERA, AND A. M. RAMOS

August 2018 saw the warmest Iberian heatwave since that of 2003. Recent climate change has exacerbated this event making it at least  $\gg 1^{\circ}\text{C}$  warmer than similar events since 1950–83.

The summer of 2018 was exceptionally warm in Europe, with outstanding temperatures over widespread non-contiguous areas, including Scandinavia, central Europe, Iberia, and the British Isles (e.g., WMO 2019). Different from other extraordinary summers, extreme temperatures did not occur during the same weeks everywhere, hitting the British Isles in June, Scandinavia and central Europe in July, and southwestern Europe in August. Together, they yielded the warmest European summer of the last 519 years, above the record-breaking summers of 2003 and 2010, albeit by a small margin, as inferred from instrumental and proxy data (Fig. 1a). Although northern and central Europe captured the attention of the media, Spain and Portugal experienced the warmest August after that of 2003

(AEMET 2019; IPMA 2019). Temperature anomalies were more pronounced during daytime over southwestern Iberia, and Portugal saw its warmest month in maximum temperature (TX) since 1931. Heat peaked during 1–7 August 2018, when an exceptional heatwave caused four (two) out of the five warmest days of the twenty-first century in Portugal (Spain), with country-mean daily TX reaching  $41.6^{\circ}\text{C}$  ( $36.4^{\circ}\text{C}$ ). We use observational and reanalysis data for 1950–2018 to quantify recent changes in the intensity of this kind of events.

**METHODS.** We describe the exceptionality (Fig. 1) and changing risk (Fig. 2) of the 2018 Iberian heatwave by using daily TX from E-OBS at  $0.25^{\circ} \times 0.25^{\circ}$  for 1950–2018 (Cornes et al. 2018) and historical series from the European Climate Assessment and Dataset (ECA&D) (Klein Tank et al. 2002) and the Instituto Português do Mar e da Atmosfera (IPMA). The atmospheric circulation is described with daily geopotential height at 500 hPa (Z500) and  $2.5^{\circ} \times 2.5^{\circ}$  from the NCEP–NCAR reanalysis (Kalnay et al. 1996). We use the analog method, which infers the probability distribution of a target field from the atmospheric circulation during the event (Stott et al. 2016, and references therein). Flow analog days are defined from their root-mean-square differences (RMSD) with the actual Z500 anomaly field over  $20^{\circ}\text{W}$ – $10^{\circ}\text{E}$ ,  $32.5^{\circ}$ – $50^{\circ}\text{N}$ . We reconstructed the Iberian ( $10^{\circ}\text{W}$ – $3.5^{\circ}\text{E}$ ,  $36^{\circ}$ – $43.5^{\circ}\text{N}$ ) mean TX by randomly picking one of the 20 best analogs for each heatwave day (1–7 August). This process was repeated 5,000 times with circulation analogs of the present (1984–2017) and past (1950–83) subperiods separately, building flow-conditioned distributions of Iberian TX for two different “worlds.” Their comparison provides the overall changes in heatwave intensity, including those due to non-anthropogenic factors [see Sánchez-Benítez et al. (2018) for details].

**AFFILIATIONS:** BARRIOPEDRO—Instituto de Geociencias, Consejo Superior de Investigaciones Científicas–Universidad Complutense de Madrid, Madrid, Spain; SOUSA AND RAMOS—Instituto Dom Luiz, Faculdade de Ciências, Universidade de Lisboa, Lisbon, Portugal; TRIGO—Instituto Dom Luiz, Faculdade de Ciências, Universidade de Lisboa, Lisbon, Portugal, and Departamento de Meteorologia, Instituto de Geociências, Universidade Federal do Rio de Janeiro, Rio de Janeiro, Brazil; GARCÍA-HERRERA—Departamento de Física de la Tierra y Astrofísica, Facultad de Ciencias Físicas, Universidad Complutense de Madrid, Madrid, Spain, and Instituto de Geociencias, Consejo Superior de Investigaciones Científicas–Universidad Complutense de Madrid, Madrid, Spain

**CORRESPONDING AUTHOR:** David Barriopedro, david.barriopedro@csic.es

DOI:10.1175/BAMS-D-19-0159.1

A supplement to this article is available online (10.1175/BAMS-D-19-0159.2)

© 2020 American Meteorological Society  
For information regarding reuse of this content and general copyright information, consult the [AMS Copyright Policy](#).

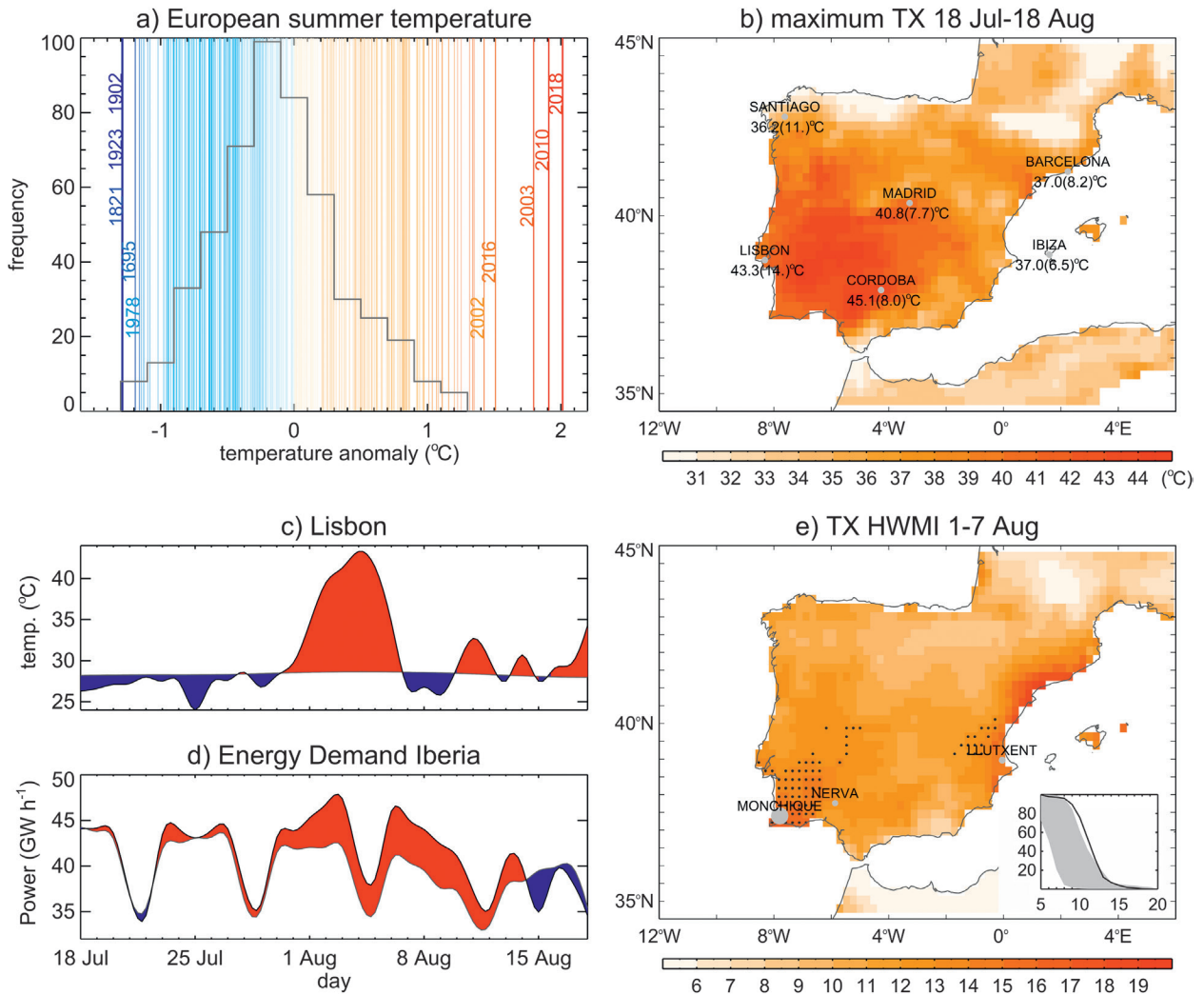


**FIG. 1.** (a) European summer land temperature anomaly ( $^{\circ}\text{C}$ ; wrt 1981–2010) over  $25^{\circ}\text{W}$ – $40^{\circ}\text{E}$ ,  $35^{\circ}$ – $70^{\circ}\text{N}$  for 1500–2018 (lines) and its 1500–2000 frequency distribution (bars) using GISS (Hansen et al. 2010) for 1901–2018 and a multi-proxy reconstruction (Luterbacher et al. 2004). (b) Warmest daily TX for 18 Jul–18 Aug 2018 (shading) and selected stations (dots), with anomalies in parentheses ( $^{\circ}\text{C}$ ; wrt 1981–2010). Daily series of (c) Lisbon TX ( $^{\circ}\text{C}$ ) and (d) maximum electricity demand for Iberia ( $\text{GW h}^{-1}$ ), with red (blue) denoting periods above (below) average (1981–2010 and week-equivalent days of 2013–17, respectively). (e) HWMI (dimensionless) for 1–7 Aug 2018 and percentage of Iberia exceeding a given value (inset plot, with the 1981–2000 5th–95th percentile range in shading). Black dots indicate record-breaking values (wrt all 7-day intervals of 18 Jul–18 Aug) and gray dots indicate major fires.

**RESULTS.** Figure 1b shows the highest TX of the 18 July–18 August 2018 period, which is close to the warmest 31-day interval of the year over Iberia. TX climbed to  $46.8^{\circ}$  and  $46.6^{\circ}\text{C}$  in weather stations of Portugal and Spain (both on 4 August), close to their national records. Although the highest TX occurred in southern and western Iberia ( $\gg 40\%$  of the Portuguese stations broke their all-time records), unprecedented temperatures were also reported in central Iberia (e.g.,  $40.8^{\circ}\text{C}$ , Madrid), the Mediterranean coast (e.g.,  $39.8^{\circ}\text{C}$ , near Barcelona), and the Balearic Islands (e.g.,  $37.0^{\circ}\text{C}$ , Ibiza). Likewise, minimum temperatures

were exceptionally high, with more than 25% of the Portuguese stations setting absolute records and some Spanish locations reporting the warmest nights of the last century (e.g.,  $25.9^{\circ}\text{C}$ , Madrid). Tropical nights affected 50% of Portugal and extended to the Mediterranean coast (e.g.,  $>25^{\circ}\text{C}$ , Barcelona) during seven consecutive days.

The first week of August saw the warmest anomalies (Fig. 2a, shading), as illustrated by the time series of Lisbon (Fig. 1c), where TX surpassed  $40^{\circ}\text{C}$  for three days, breaking its previous record twice by a large margin ( $\gg 2^{\circ}\text{C}$  of exceedance). The atmospheric



of population in major touristic destinations, where the heat persisted the most. According to the Heat-wave Magnitude Intensity (HWMI) index [Russo et al. 2015; also see the online supplemental material (SM)], more than half of Iberia experienced extreme HWMI values (unprecedented in the southern half of Portugal and some Mediterranean areas; Fig. 1e), resulting in the most intense Iberian heatwave on 7-day time scales since 1950 after the 2003 episode (Table ES1).

Figure 2b shows the distribution of Iberian TX averaged for the heatwave period, as inferred from flow analogs of the past (blue boxplot) and present (red) climate. Present-day analogs explain almost 60% of the observed Iberian TX, the remaining being attributed to non-dynamical processes (e.g., feedbacks) and limited sampling. The comparison reveals that similar atmospheric conditions trigger warmer Iberian TX ( $\gg 1^\circ\text{C}$ ) now than in the recent past (i.e., the observed circulation would have caused a less severe heatwave in the past). This agrees with a warming and poleward trend of 2018-like Saharan intrusions, as reconstructed from flow analogs (see Fig. ES1 in the SM). Figure 2d quantifies how recent trends have changed the intensity of these Iberian heatwaves, by counting the fraction of replicated analogs with 7-day mean Iberian TX above a certain threshold in each subperiod. The flow-conditioned probability of experiencing Iberian heatwaves with TX anomalies above  $\gg 2.5^\circ\text{C}$  has doubled in just 35 years, equivalent to a fraction of attributable risk (FAR) of  $\gg 0.5$  (see the SM). Under the atmospheric circulation conditions of the 2018 heatwave, the chances of exceeding  $3^\circ\text{C}$  have risen by more than five times (FAR of 0.8).

**CONCLUSIONS AND DISCUSSION.** As the atmospheric circulation is constrained, the reported FAR should be attributed to thermodynamical changes (warming trend). However, flow analogs of the 2018 event show significant differences between the two subperiods, displaying smaller RMSD in the present than in the past (gray boxplots, Fig. 2b). Figure 2c (black line) confirms a significant ( $p < 0.05$ ) upward trend in the 1950–2018 frequency series of “good” flow analogs, defined as those days with RMSD below the 5th percentile of the event distribution. This trend may reflect dynamical (e.g., Z500 gradients) changes or thermodynamical effects (e.g., thermal Z500 rise). To address this, we repeated the analysis by removing the regional monthly mean trends of Z500 and TX. The resulting thermodynamically adjusted (TA) distributions for the two subperiods become much closer and the trend in the number of

good flow analogs is no longer significant at  $p < 0.05$  (gray line, Fig. 2c). Their difference has been added to the past distribution to estimate the contribution of dynamical changes (green line, Fig. 2d). Dynamical changes cannot explain the changing risk of Iberian TX anomalies. Therefore, regional warming is largely responsible for the FAR, particularly in the higher TX thresholds. Further studies are encouraged to pin down the key drivers and their contributing roles to the reported changes (e.g., land–atmosphere feedbacks).

**ACKNOWLEDGMENTS.** We acknowledge the E-OBS dataset from <http://www.uerra.eu> (EU-FP6), the Copernicus Climate Change Service, the data providers in ECA&D (<https://www.ecad.eu>), IPMA, the GISTEMP Team 2019 dataset ([data.giss.nasa.gov/gistemp/](http://data.giss.nasa.gov/gistemp/)) and J. Luterbacher for providing the proxy-based reconstruction. Energy data were retrieved from <https://demanda.ree.es/> and <http://www.centrodeinformacao.ren.pt>. AMR, PMS, and RMT were supported by project IMDROFLOOD (Improving Drought and Flood Early Warning, Forecasting and Mitigation using real-time hydroclimatic indicators; WaterJPI/0004/2014) through Fundação para a Ciência e a Tecnologia (FCT), Portugal. AMR was also supported by the Scientific Employment Stimulus 2017 from FCT (CEECIND/00027/2017). We thank three reviewers for their comments.

## REFERENCES

- AEMET, 2019: Resúmenes Climatológicos: Agosto de 2018. Agencia Estatal de Meteorología, accessed 5 January 2019, 11 pp., [http://www.aemet.es/documentos/es/serviciosclimaticos/vigilancia\\_clima/resumenes\\_climat/mensuales/2018/res\\_mens\\_clim\\_2018\\_08.pdf](http://www.aemet.es/documentos/es/serviciosclimaticos/vigilancia_clima/resumenes_climat/mensuales/2018/res_mens_clim_2018_08.pdf).
- Cornes, R., G. van der Schrier, E. J. M. van den Besselaar, and P. D. Jones, 2018: An ensemble version of the E-OBS temperature and precipitation datasets. *J. Geophys. Res. Atmos.*, **123**, 9391–9409, <https://doi.org/10.1029/2017JD028200>.
- Hansen, J., R. Ruedy, M. Sato, and K. Lo, 2010: Global surface temperature change. *Rev. Geophys.*, **48**, RG4004, <https://doi.org/10.1029/2010RG000345>.
- IPMA, 2019: Boletim Climatológico: Agosto 2018, Portugal continental. Instituto Português do Mar e da Atmosfera, accessed 5 January 2019, 16 pp., [http://www.ipma.pt/recursos/www/docs/im.publicacoes/edicoes.online/20180924/QtyZvZwgxxBnLFiHk-SkX/cli\\_20180801\\_20180831\\_pcl\\_mm\\_co\\_pt.pdf](http://www.ipma.pt/recursos/www/docs/im.publicacoes/edicoes.online/20180924/QtyZvZwgxxBnLFiHk-SkX/cli_20180801_20180831_pcl_mm_co_pt.pdf).
- Kalnay, E., and Coauthors, 1996: The NCEP/NCAR 40-Year Reanalysis Project. *Bull. Amer. Meteor.*

- Soc.*, **77**, 437–471, [https://doi.org/10.1175/1520-0477\(1996\)077<0437:TNYRP>2.0.CO;2](https://doi.org/10.1175/1520-0477(1996)077<0437:TNYRP>2.0.CO;2).
- Klein Tank, A. M. G., and Coauthors, 2002: Daily dataset of 20th-century surface air temperature and precipitation series for the European Climate Assessment. *Int. J. Climatol.*, **22**, 1441–1453, <https://doi.org/10.1002/joc.773>.
- Luterbacher, J., D. Dietrich, E. Xoplaki, M. Grosjean, and H. Wanner, 2004: European seasonal and annual temperature variability, trends, and extremes since 1500. *Science*, **303**, 1499–1503, <https://doi.org/10.1126/science.1093877>.
- Russo, S., J. Sillmann, and E. Fischer, 2015: Top ten European heatwaves since 1950 and their occurrence in the coming decades. *Environ. Res. Lett.*, **10**, 124003, <https://doi.org/10.1088/1748-9326/10/12/124003>.
- Sánchez-Benítez, A., R. García-Herrera, D. Barriopedro, P. M. Sousa, and R. M. Trigo, 2018: June 2017: The earliest mega-heatwave of reanalysis period. *Geophys. Res. Lett.*, **45**, 1955–1962, <https://doi.org/10.1002/2018GL077253>.
- San-Miguel-Ayanz, J., and Coauthors, 2019: Advance EFFIS Report on Forest Fires in Europe, Middle East and North Africa 2018. EUR 29722 EN, Joint Research Centre, 36 pp., <https://doi.org/10.2760/262459>.
- Sousa, P. M., D. Barriopedro, A. M. Ramos, R. García-Herrera, F. Espírito-Santo, and R. M. Trigo, 2019: Saharan air intrusions as a relevant mechanism for Iberian heatwaves: The record breaking events of August 2018 and June 2019. *Wea. Climate Extremes*, **26**, 100224, <https://doi.org/10.1016/j.wace.2019.100224>.
- Stott, P. A., and Coauthors, 2016: Attribution of extreme weather and climate-related events. *Wiley Interdiscip. Rev.: Climate Change*, **7**, 23–41, <https://doi.org/10.1002/wcc.380>.
- WMO, 2019: WMO Statement on the State of the Global Climate in 2018. WMO-No. 1233, World Meteorological Organization, 39 pp., [https://library.wmo.int/doc\\_num.php?explnum\\_id=5789](https://library.wmo.int/doc_num.php?explnum_id=5789).

